Young's Modulus Measurements in Standard IC CMOS Processes Using MEMS Test Structures

Janet C. Marshall, David L. Herman, P. Thomas Vernier, *Member, IEEE*,
Don L. DeVoe, and Michael Gaitan, *Senior Member, IEEE*

***Abstract*—This letter[1] presents a method to measure the Young's moduli of individual thin-film layers in a commercial integrated circuit (IC) foundry process. The method is based on measuring the resonance frequency of an array of micromachined cantilevers and using the presented optimization analysis to determine the elastic modulus of each layer. Arrays of cantilever test structures were fabricated in a commercial CMOS IC process and were released using XeF_2 as a postprocessing etch. A piezoelectric transducer placed under the test chip was used to excite the cantilevers to resonance, and the resonance frequency was measured using a laser Doppler vibrometer. It is reported that excellent agreement for values of Young's modulus is observed for cantilevers between 200 and 400 μm in length, with average standard deviation being 4.07 GPa.**

***Index Terms*—CMOS, MEMS, residual stress, resonance, test structures, thickness measurements, Young's modulus.**

I. Introduction

HIGH VALUES of residual stress can initiate failure mechanisms in integrated circuits (ICs) such as electromigration, stress migration, and delamination [1], and thus, methods for its characterization are of interest for IC process development and monitoring. Residual stress of thin films is typically measured by wafer curvature [2] or X-ray diffraction [3]. However, these methods are not easily extended to multilayer films and cannot be used for small specimens. An on-chip method has recently been standardized to measure residual strain [4], but this still requires the measurement of Young's modulus to determine the residual stress. In [5], published values for Young's modulus were used to determine the residual stress of films from strain measurements. However, it would be more desirable to directly measure the Young's modulus on-chip due to the percent difference, of the extreme values obtained from a material-property database [6], ranging from 45% [7] to 114% [8] for this value.

Tensile stress methods have been developed to measure the Young's modulus of thin films on small specimens [9], and the resulting values can differ substantially from bulk-material measurements, depending on the process parameters and methods used to create the films. What is still lacking is an on-chip method that is compatible with test methods using rapid wafer prober techniques. One likely candidate for on-chip wafer prober-compatible measurements is based on mechanical resonance. Previously, researchers have used thin-film cantilever resonators to determine the Young's moduli of materials in single-layered [10] and dual-layered [11] structures, but this approach has not been extended to measure the Young's moduli of thin films in CMOS processes due to the complexity of the approach coupled with the inability to obtain believable results.

This letter presents a relatively simple and successful method of determining the Young's moduli of the layers in a CMOS process. It uses multilayered micromachined cantilevers that are excited to resonance and are measured using a laser Doppler vibrometer (LDV). The resonance frequency predicted by a composite-beam model is used to extract the Young's moduli of all the individual thin-film layers in the cantilever. A three-step optimization technique is used to obtain the Young's moduli of all the layers in 16 independently designed cantilevers. From the results, the Young's moduli of all the thin-film layers in the CMOS process are determined.

II. Composite-Beam Analysis

The undamped natural frequency of a uniform thin slender cantilever is a function of its geometry, density, elasticity, and boundary conditions, and it is expressed as [12], [13]

$$f = \frac{\lambda^2}{2\pi L^2}\sqrt{\frac{EI}{m}} \tag{1}$$

where E, I, m, and L are the Young's modulus, the area moment of inertia about the neutral axis, the mass per unit length, and the length of the beam, respectively. The eigenvalue, λ, accounts for the effects of the boundary conditions, such that $\lambda \approx 1.875$ for a clamped-free beam in its first natural mode of vibration.

For a multilayered structure, the bending stiffness, EI, and the linear density, m, in (1) are defined by the summation of the

Manuscript received July 3, 2007; revised August 7, 2007. This work was supported in part by the National Institute of Standards and Technology (NIST) Office of Microelectronics Programs. The review of this letter was arranged by Editor Y. Taur.

J. C. Marshall, D. L. Herman, and M. Gaitan are with the Semiconductor Electronics Division, National Institute of Standards and Technology (NIST), Gaithersburg, MD 20899 USA (e-mail: janet.marshall@nist.gov).

P. T. Vernier is with the MOSIS Service, Information Sciences Institute, Viterbi School of Engineering, University of Southern California, Marina del Rey, CA 90292 USA (e-mail: vernier@mosis.com).

D. L. DeVoe is with the University of Maryland, College Park, MD 20742 USA (e-mail: ddev@eng.umd.edu).

Digital Object Identifier 10.1109/LED.2007.906460

[1]Contribution of the National Institute of Standards and Technology (NIST); not subject to copyright.

individual terms for each layer in the beam as follows:

$$\overline{EI} = \sum_{i=1}^{N} E_i I_i \qquad \text{and} \qquad \overline{m} = \sum_{i=1}^{N} m_i \tag{2}$$

where the barred symbols represent composite values, N is the total number of layers in the beams' cross section, and I_i, as an example, is equal to the area moment of inertia of the ith layer with respect to the neutral axis of the beam, which is a function of E_i. Expressing the Young's moduli and area moments of inertia as vectors in (1) can be done using $E = [E_1, E_2, \ldots, E_N]$ and $I(E) = [I_1, I_2, \ldots, I_N]^{\mathrm{T}}$.

To extract the Young's moduli contained in the vector E from the measured resonance frequency, f_m, of a cantilever with N layers, an optimization approach defines a function

$$d = \left| f_m^2 - f^2(E) \right| \tag{3}$$

where $f(E)$ is the result obtained in (1) using $\overline{m}$ and the vectors for E and I. A local minimum value for d is found using an unconstrained nonlinear optimization, which yields the Young's moduli in the vector, E, that most closely fit the squared measured frequency f_m^2.

III. Test Structure Fabrication and Measurement

Cantilever test structures were fabricated on three separate processing runs in a 1.5-μm commercial CMOS foundry process available through the MOSIS Service.[2] The process includes two polysilicon and two aluminum interconnect layers sandwiched between layers of insulating silicon dioxide. An array consisted of 16 cantilever test structures of the same length, each with a unique set of interconnects as indicated in the four interconnect columns of Table I. For example, for cantilever #10, a Young's modulus value is given for poly1, E_{p1}, and metal2, E_{m2}; thus, those two interconnects are included in that cantilever. Seven cantilever arrays (six of different lengths) were measured.

The cantilever test structures were released using an isotropic XeF_2 etch [15], which removes the silicon around and beneath each cantilever.

For measurement, the test chip is attached to a small piezoelectric transducer that is used to mechanically excite the entire chip, thereby driving the test structures through base excitation. This transducer receives an excitation signal from a function generator, and an LDV is used to measure the cantilever's frequency response. The resonance frequency is easily identified by locating the peak of the response plotted as a function of excitation frequency. For 500-μm-long and 40-μm-wide cantilevers, resonance frequencies for the 16 cantilevers are given in Table I.

The film thickness is an important parameter in this measurement. A second type of test structure was included on the chip to determine layer thicknesses. These thickness test structures, as shown in Fig. 1(a), consist of a series of steps, such as that shown in the cross section in Fig. 1(b), that is created by the presence or absence of process layers. The arrows in the figures indicate where step-height measurements [16] are taken with an optical interferometer. Given the knowledge of the layers comprising the steps, thickness values were determined [17]. The thicknesses, as calculated from the step-height measurements, were compared with thicknesses obtained from MOSIS-supplied capacitance and sheet-resistance values in order to obtain the thickness with the smallest combined standard uncertainty value [14] for use in the Young's modulus calculations. Consult [17] for more details and representative thickness values. Table I includes thicknesses for the layers in the first cantilever t_1.

IV. Young's Modulus Results

The optimization method requires initial estimates (E_{ini}) for the Young's moduli. As given in Table I, these were obtained from [6] for field oxide (E_{fo}), thermal oxide (E_{th}), deposited oxide (E_{de}), glass (E_{gl}), nitride cap (E_{ni}), first polysilicon layer (E_{p1}), second polysilicon layer (E_{p2}), first metal layer (E_{m1}), and second metal layer (E_{m2}).

The optimization consisted of three parts. First, the cantilever consisting of only oxides was optimized to find the Young's moduli of those layers. Second, the resulting Young's moduli from the first step were used as starting values in the four cantilevers that had only one interconnect layer encompassed in oxide. Finally, the optimized values for the above five optimizations were then averaged, and the averages were used as starting values in the optimization of all 16 cantilevers, which were optimized one by one.[3]

There were three separate design submissions to the MOSIS. For each submission, resonance-frequency data from one test chip were obtained. The first and second submissions had cantilever arrays of 500 μm in length. The third submission had cantilever arrays of 100, 148, 200, 300, and 400 μm in length. The data in Fig. 2 average the results from the first two submissions for $L = 500$ μm. The data from the first submission are given in Table I. For this submission, unlike the others, there was a nitride cap on top of the glass layer. In addition, it is noteworthy that the Young's moduli for the other layers from this chip are comparable to the Young's moduli from the other submissions, which are to be presented next.

Representative plots of Young's modulus (E_{av} from Table I for the 16 cantilevers) versus cantilever length are given in Fig. 2 for the poly1, the deposited oxide, and the metal1. The error bars correspond to the standard deviations, σ, such as those found in Table I for the 16 cantilevers. The average Young's modulus value as a function of length, E_L, and the standard deviation, σ_{EL}, are given in the legend. For the σ_{EL} data in Table I from $L = 200$ μm to $L = 400$ μm, inclusive, the average of the σ_{EL} values is 4.07 GPa, and the average value for u_c is 5.24 GPa for the $L = 500$ μm data. These data and the

[2]In this letter, commercial instruments or processes may be identified. This does not imply recommendation or endorsement by NIST nor does it imply that the instruments or processes are the best available for the purpose.

[3]The optimization results are dependent upon the initial estimates. Obtaining starting values in the manner described produced believable results in comparison to other attempts. This does not imply that the method described is the only possible route or that the unconstrained nonlinear optimization is the only possible optimization method.

TABLE I
REPRESENTATIVE YOUNG'S MODULUS (IN GIGAPASCAL) AND FREQUENCY MEASUREMENTS ($L = 500\ \mu$m, $W = 40\ \mu$m[a])

	Oxide Layers					Interconnects				f_m
#	E_{fo}	E_{th}	E_{de}	E_{gl}	E_{ni}	E_{p1}	E_{p2}	E_{m1}	E_{m2}	(kHz)
1	60.4		76.7	56.7	163.7					13.05
2	65.3		73.0	51.0	196.4	176.2				15.01
3	64.2		73.5	53.7	189.1		180.7			15.00
4	66.9	66.7	71.5	54.4	202.9	172.6	171.6			16.76
5	67.3		77.0	53.2	207.1			57.3		15.52
6	63.0		74.0	54.2	181.5	169.2		61.7		17.45
7	62.6		74.5	53.8	159.8		183.9	64.0		17.62
8	63.3	70.2	73.1	54.2	158.9	169.5	184.0	64.2		19.12
9	63.0		71.9	55.0	169.6				74.0	16.59
10	62.4		75.0	53.4	163.7	173.5			73.9	18.62
11	62.7		74.6	54.0	181.9		177.0		71.7	18.77
12	63.6	70.1	73.9	53.6	179.0	171.8	180.0		70.8	20.34
13	65.5		74.8	53.9	200.1			56.6	70.7	19.18
14	62.0		75.3	55.6	147.3	173.0		65.7	71.8	20.73
15	62.4		77.5	56.0	130.8		180.7	67.5	70.9	21.00
16	62.2	75.7	76.6	54.8	128.6	173.0	187.5	59.8	71.0	22.56
t_1[b]	0.69		1.48	0.53	0.53					–
ρ[c]	2.20	2.20	2.20	2.25	3.10	2.33	2.33	2.70	2.70	–
E_{ini}	69.0	69.0	69.0	51.5	180.0	165.0	165.0	70.0	70.0	–
E_{av}	63.5	70.7	74.6	54.2	172.5	172.3	180.7	62.1	71.8	–
σ	1.9	3.7	1.8	1.3	24.2	2.2	4.9	3.9	1.4	–
σ_{EL}[d]	3.81	0.71	3.67	0.67	–	10.90	10.24	1.92	0.63	–
u_c[e]	4.3	3.8	4.1	1.5	–	11.1	11.4	4.3	1.5	–
E_{lo}	46	46	46	46	104	120	120	47	47	–
E_{hi}	92	92	92	92	380	210	210	74	74	–

[a] The width includes two 3.2 μm oxide borders.
[b] The layer thicknesses in the first cantilever, t_1, are given in micrometers.
[c] The density, ρ, is given in grams per cubic centimeter.
[d] These data are for L=200 μm to L=400 μm, inclusive.
[e] Here, *it is assumed* that the combined standard uncertainty values [14], u_c, are due solely to beam construction and estimated beam length variations, such that $u_c = (\sigma^2 + \sigma_{EL}^2)^{1/2}$ with a coverage factor k=3.

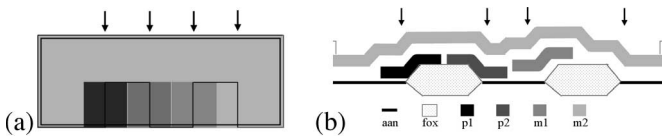

Fig. 1. Design and cross section of a thickness test structure.

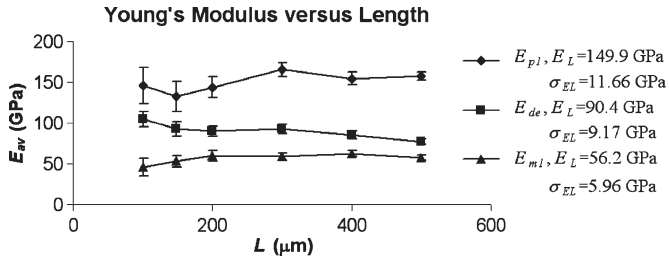

Fig. 2. Optimized Young's moduli for poly1, deposited oxide, and metal1 versus cantilever length.

plots reveal that overall, the results are relatively independent of length, and the Young's moduli are consistent with the lower bounds, $E_{\rm lo}$, and the upper bounds, $E_{\rm hi}$, for this parameter as given in the material-property database [6] and as included in Table I.

V. CONCLUSION

A method for determining the Young's moduli of the various thin-film layers in a commercial CMOS process has been presented. A composite-beam model derived from simple thin-beam theory was successfully used to analyze the response of multilayer cantilevers. Given the cantilever dimensions, the layer thicknesses, and the resonance frequencies, a three-step optimization approach was used to find the resulting Young's

moduli. These results are in agreement with published values using other measurement methods. These newly acquired Young's modulus values can be used in conjunction with residual-strain measurements to obtain the residual-stress values of the thin-film layers in order to improve the yield in CMOS fabrication processes.

ACKNOWLEDGMENT

The authors would like to thank the following people from the National Institute of Standards and Technology (NIST) for reviewing this letter: Dr. C. McGray, R. Allen, Dr. D. Read, E. Secula, Dr. D. Seiler, and R. Thurber. The authors would also like to thank P. Kangavari and J. Huang for sample preparation and selected measurements performed at NIST.

REFERENCES

[1] *Mitsubishi Semiconductors Reliability Handbook*, Semiconductor Marketing Div., Mitsubishi Electric Corp., Tokyo, Japan, Feb. 1992.

[2] P. A. Flinn *et al.*, "Measurement and interpretation of stress in aluminum-based metallization as a function of thermal history," *IEEE Trans. Electron Devices*, vol. ED-34, no. 3, pp. 689–699, Mar. 1987.

[3] D. Zeng *et al.*, "Residual stress and strain in CdZnTe wafer examined by X-ray diffraction methods," *Appl. Phys. A, Solids Surf.*, vol. 86, no. 2, pp. 257–260, Feb. 2007.

[4] ASTM E08, "E 2245 standard test method for residual strain measurements of thin, reflecting films using an optical interferometer," *Annual Book of ASTM Standards*, vol. 03.01, 2006.

[5] S. A. Smee *et al.*, "IC test structures for multilayer interconnect stress determination," *IEEE Electron Device Lett.*, vol. 21, no. 1, pp. 12–14, Jan. 2000.

[6] MEMS and Nanotechnology Clearinghouse, MEMS and Nanotechnology Exchange. [Online]. Available: http://www.memsnet.org/material

[7] M. Chinmulgund *et al.*, "Effect of Ar gas pressure on growth, structure, and mechanical properties of sputtered Ti, Al, TiAl, and Ti_3Al films," *Thin Solid Films*, vol. 270, no. 1/2, pp. 260–263, Dec. 1995.

[8] B. Halg, "On a nonvolatile memory cell based on micro-electromechanics," in *Proc. IEEE Micro Electro Mech. Syst. Workshop*, Napa Valley, CA, Feb. 1990, pp. 172–176.

[9] W. N. Sharpe, Jr. and K. Jackson, "Tensile testing of MEMS materials," in *Proc. Microscale Syst.: Mech. Meas. Symp.*, 2000, pp. ix–xiv.

[10] L. Kiesewetter *et al.*, "Determination of Young's moduli of micromechanical thin films using the resonance method," *Sens. Actuators A, Phys.*, vol. 35, no. 2, pp. 153–159, Dec. 1992.

[11] K. E. Petersen and C. R. Guarnieri, "Young's modulus measurements of thin films using micromechanics," *J. Appl. Phys.*, vol. 50, no. 11, pp. 6761–6766, Nov. 1979.

[12] C. F. Beards, *Structural Vibration Analysis: Modeling, Analysis and Damping of Vibrating Structures*. New York: Wiley, 1983.

[13] I. Voiculescu *et al.*, "Electrostatically actuated resonant microcantilever beam in CMOS technology for the detection of chemical weapons," *IEEE Sensors J.*, vol. 5, no. 4, pp. 641–647, Aug. 2005.

[14] B. N. Taylor and C. E. Kuyatt, "Guidelines for evaluating and expressing the uncertainty of NIST Measurement Results," NIST, Gaithersburg, MD, NIST Technical Note 1297, 1994.

[15] F. Chang *et al.*, "Gas-phase silicon micromachining with xenon difluoride," in *Proc. SPIE Symp. Micromach. Microfab.*, Austin, TX, 1995, pp. 117–128.

[16] SEMI MS2-0307, *Test Method for Step-Height Measurements of Thin, Reflecting Films Using an Optical Interferometer*. [Online]. Available: http://www.semi.org/

[17] J. C. Marshall and P. T. Vernier, "Electro-physical technique for post-fabrication measurements of CMOS process layer thicknesses," *NIST J. Res.*, vol. 112, no. 4, 2007. in press.